HUMAN MUTATION 29(5), 757–764, 2008

METHODS

High-Throughput Amplicon Scanning of the TP53 Gene in Breast Cancer Using High-Resolution Fluorescent Melting Curve Analyses and Automatic Mutation Calling

Roy Bastien,[1] Tracey B. Lewis,[2] Jason E. Hawkes,[1] John F. Quackenbush,[1] Thomas C. Robbins,[3] Juan Palazzo,[4] Charles M. Perou,[5,6] and Philip S. Bernard[1,2]*

[1]Department of Pathology, University of Utah School of Medicine, Salt Lake City, Utah; [2]The ARUP Institute for Clinical and Experimental Pathology, Salt Lake City, Utah; [3]Idaho Technology, Inc., Salt Lake City, Utah; [4]Department of Pathology, Thomas Jefferson University, Philadelphia, Pennsylvania; [5]Department of Genetics, Lineberger Comprehensive Cancer Center, University of North Carolina at Chapel Hill, Chapel Hill, North Carolina; [6]Department of Pathology & Laboratory Sciences, Lineberger Comprehensive Cancer Center, University of North Carolina at Chapel Hill, Chapel Hill, North Carolina

Communicated by Ian N.M. Day

Identifying mutations in the TP53 gene is important for cancer prognosis, predicting response to therapy, and determining genetic risk. We have developed a high-throughput scanning assay with automatic calling to detect TP53 mutations in DNA from fresh frozen (FF) and formalin-fixed paraffin-embedded (FFPE) tissues. The coding region of the TP53 gene (exons 2–11) was PCR-amplified from breast cancer samples and scanned by high-resolution fluorescent melting curve analyses using a 384-well format in the LightCycler 480 instrument. Mutations were confirmed by direct sequencing. Sensitivity and specificity of scanning and automatic mutation calling was determined for FF tissue (whole genome amplified [WGA] and non-WGA) and FFPE tissue. Thresholds for automatic mutation calling were established for each preparation type. Overall, we confirmed 27 TP53 mutations in 68 primary breast cancers analyzed by high-resolution melting curve scanning and direct sequencing. Using scanning and automatic calling, there was high specificity (>95%) across all DNA preparation methods. Sensitivities ranged from 100% in non-WGA DNA from fresh tissue to 86% in WGA DNA and DNA from formalin-fixed, paraffin-embedded tissue. Scanning could detect mutated DNA at a dilution of 1:200 in a background of wild-type DNA. Mutation scanning by high-resolution fluorescent melting curve analyses can be done in a high-throughput and automated fashion. The TP53 scanning assay can be performed from a variety of specimen types with high sensitivity/specificity and could be used for clinical and research purposes. Hum Mutat 29(5), 757–764, 2008.

KEY WORDS: high-throughput; scanning; high-resolution melting; automatic calling; TP53

INTRODUCTION

TP53 (MIM# 191170) encodes a multifunctional transcription factor involved in cell proliferation, genomic stability, and cell death [Hollstein et al., 1991; Levine, 1997; Levine et al., 1991]. Mutations in TP53 occur both in sporadic cancers and familial cancers such as Li-Fraumeni and Li-Fraumeni-like syndromes [Hollstein et al., 1991; Malkin et al., 1990; Santibanez-Koref et al., 1991]. Additional sporadic cancers found to have frequent TP53 somatic mutations are ovarian, colorectal, and tumors of the aerodigestive tract including the esophagus, head and neck, and lung [Olivier et al., 2002]. In contrast, germline TP53 mutations most frequently give rise to breast cancer, adrenal cancer, sarcomas, and brain cancer.

Alterations in TP53 can occur throughout the coding region (exons 2–11) and at intron–exon boundaries [Hainaut and Hollstein, 2000]. The majority of TP53 mutations are missense substitutions (75%) within the DNA binding domain (exons 5–8) causing loss of transactivation functions [Ory et al., 1994; Pavletich et al., 1993; Petitjean et al., 2007a, 2007b]. In sporadic cancer, about 25% of the mutations are found at highly mutable hotspots within codons 175, 245, 248, 249, 273, and 282 [Olivier et al., 2002] while the vast majority of mutations are distributed along the gene.

The Supplementary Material referred to in this article can be accessed at http://www.interscience.wiley.com/jpages/1059-7794/suppmat.

Received 30 September 2007; accepted revised manuscript 12 December 2007.

*Correspondence to: Philip S. Bernard, Pathology, University of Utah, Huntsman Cancer Institute, 2000 Circle of Hope, Salt Lake City, UT 84112-5550. E-mail: phil.bernard@hci.utah.edu

Grant sponsors: ARUP Institute for Clinical and Experimental Pathology; National Cancer Institute (NCI); Grant number: R33-CA97769-01 P50-CA58223-09A1.

DOI 10.1002/humu.20726

Published online 17 March 2008 in Wiley InterScience (www.interscience.wiley.com).

Approximately 25% of breast cancers harbor a TP53 mutation, although the prevalence changes depending on the population, stage of disease, and particular molecular subtype [Borresen-Dale, 2003; Olivier et al., 2002; Sorlie et al., 2001]. TP53 mutations in breast cancer have been associated with aggressive histological features, poor prognosis, and resistance to therapy [Aas et al., 1996; Allred et al., 1993; Bergh et al., 1995; Berns et al., 2000; Borresen-Dale, 2003; Geisler et al., 2001, 2003; Olivier et al., 2006; Soong et al., 1997]. Despite its strong prognostic significance in breast cancer and other cancers [Olivier et al., 2002; Petitjean et al., 2007a], clinical testing for sporadic TP53 mutations in solid/soft tumors is rarely performed. This is in part due to nonsupportive data from studies associating outcome to p53 mutation status as scored by protein immunohistochemistry [Elledge et al., 1995; MacGrogan et al., 1996; Rozan et al., 1998]. However, immunohistochemistry may miss as many as 30% of TP53 gene mutations (mainly nonsense type) because only mutations resulting in protein nuclear retention (mainly missense type) are scored positive [Legros et al., 1994]. Direct sequencing has been more predictive for outcome and therapy response in breast cancer [Bergh et al., 1995; Berns et al., 2000; Geisler et al., 2001; Soussi and Beroud, 2001].

With over 22,000 somatic mutations reported in the TP53 gene, it has been difficult to sort out the functional and therapeutic significance of each alteration [Petitjean et al., 2007a, 2007b]. There have been a range of methods employed to scan the TP53 gene sequence including conventional denaturant slab gels [Borresen et al., 1991], fluorescence-based single-strand conformation polymorphism [Moore et al., 2000], fluorescent melting curve analyses [Krypuy et al., 2007; Millward et al., 2002], temporal temperature gradient gel electrophoresis [Sorlie et al., 2005], and array-based methods [Ahrendt et al., 1999; Le Calvez et al., 2005; Tonisson et al., 2002; Wikman et al., 2000]. Microarray analysis has also been used to infer p53 functional status by gene expression [Miller et al., 2005], since alterations in other genes could effectively result in a null p53 phenotype (e.g., amplification of MDM2).

In this work, we apply recent advancements in instrumentation, reagents, and software to scan the coding region of TP53 (exons 2–11) in breast cancer by high-resolution fluorescent melting curve analyses. Using the LightCycler 480 (LC480; Roche Diagnostics Corporation, Indianapolis, IN), we show that this can be done in an automated, high-throughput fashion using fresh frozen (FF) tissue, formalin-fixed paraffin-embedded (FFPE) tissue, and whole genome amplified (WGA) DNA.

MATERIALS AND METHODS

Sample Procurement and DNA Extraction

All samples used in this study were collected and handled in compliance with federal and institutional guidelines. A total of 68 primary breast cancer samples, three corresponding lymph node metastases, and three normal breast samples from reduction mammoplasty were procured as FF tissue in the Departments of Pathology at the University of Utah and Thomas Jefferson University. Samples were flash frozen in liquid nitrogen and stored at –80°C. DNA from three cell lines (MCF7, SKBR3, and BT474) were used as controls (ATCC, Manassas, VA). Total DNA from FF samples and cell lines was isolated using the Qiagen DNeasy kit (Valencia, CA) following the manufacturer's instructions.

Hematoxylin and eosin (H&E) slides were used to confirm the presence of cancer (>20%) in each FFPE tissue block. Sections of 10 microns were cut from the FFPE tissue blocks and deparaffinized in Hemo-De (Scientific Safety Solvents, Keller, TX) and then washed with 100% ethanol. FFPE DNA was isolated using the Gentra Puregene kit (Gentra Systems, Minneapolis, MN). All DNA stocks were stored at –80°C.

TABLE 1. **Optimal Grouping Sensitivity for Automatic Mutation Scanning in DNA From Different Sample Preparations***

	Grouping sensitivity thresholds		
Fresh frozen[a]	0.20	0.15	0.10
True positives	**7**	6	5
True negatives	**283**	285	286
False positives	**4**	2	1
False negatives	**0**	1	2
Total amplicons	**294**	294	294
Sensitivity	**1.00**	0.86	0.71
Specificity	**0.99**	0.99	1.00
Fresh frozen WGA[a]	0.20	0.15	0.10
True positives	6	**6**	4
True negatives	266	**274**	283
False positives	21	**13**	4
False negatives	1	**1**	3
Total amplicons	294	**294**	294
Sensitivity	0.86	**0.86**	0.57
Specificity	0.93	**0.95**	0.99
FFPE[a]	0.20	0.15	0.10
True positives	6	**6**	5
True negatives	268	**287**	287
False positives	19	**0**	0
False negatives	1	**1**	2
Total amplicons	294	**294**	294
Sensitivity	0.86	**0.86**	0.71
Specificity	0.93	**1.00**	1.00
Fresh frozen[b]	0.20	0.15	0.10
True positives	**12**	11	11
True negatives	**467**	469	470
False positives	**4**	2	1
False negatives	**0**	1	1
Total amplicons	**483**	483	483
Sensitivity	**1.00**	0.92	0.92
Specificity	**0.99**	1.00	1.00

*Bold indicates "group sensitivities."
[a]Comparing 14 samples across three preparation methods.
[b]Calculated from 23 samples with complete sequencing.

Whole Genomic Amplification

Whole genome amplification from FF samples was done using the GenomePlex™ Complete Whole Genome Amplification Kit (Sigma, St. Louis, MO) and following the manufacturer's instructions. Each sample was amplified in triplicate and then pooled for scanning to reduce variability.

Primer Design

Primers for TP53 were designed from the NCBI RefSeq NM_000546.3 (www.ncbi.nlm.nih.gov/RefSeq) and using Primer Design 5 (Scientific and Educational Software, Cary, NC). Amplicons were designed between 80 and 150 bp in length for scanning and longer amplicons (>200 bp) were designed for direct sequencing from fresh tissue DNA. Lyophilized primers (Operon Inc., Huntsville, AL) were resuspended in 10 mM Tris-HCl (pH 8.3) and 0.1 mM EDTA to a final concentration of 60 μM and stored at–80°C. Primer sequences for scanning and sequencing are presented in Supplementary Tables S1 and S2, respectively (available online at http://www.interscience.wiley.com/jpages/1059-7794/suppmat).

Real-Time PCR and Fluorescent Melting Curves

PCR amplification was carried out on the LightCycler 480(Roche Diagnostics Corporation). Each reaction contained 2 μl DNA (10 ng) and 8 μl of PCR master mix with the following

final concentration of reagents: 0.5 × Titanium Taq, 50 mM Tris-HCl (pH 8.3), 100 ng/μl bovine serum albumin (BSA), 3 mM $MgCl_2$, 0.2 mM dATP, 0.2 mM dCTP, 0.2 mM dGTP, 0.6 mM 2′-deoxyuridine 5′-triphosphate (dUTP), 1 × LC Green Plus dye (Idaho Technology, Salt Lake City, UT), and 0.4 μM of both forward and reverse primers for the selected target. The PCR was done with an initial denaturation step at 94°C for 2 min and then 45 cycles of denaturation (94°C for 2 s), annealing (57°C for 6 s), and extension (72°C for 6 s). Fluorescence acquisition (530 nm) was taken once each cycle at the end of the extension phase. The crossing point (Cp) for each reaction is the fractional cycle number at which the fluorescence signal from the accumulating PCR product rises above background. After PCR, a postamplification melting curve program was initiated by heating to 94°C for 10 s, cooling to 55°C for 10 s, and increasing the temperature to 95°C while continuously measuring fluorescence at 18 acquisitions per degree. Each PCR run contained a negative (no template) control and each amplicon done in triplicate.

Amplicon Scanning and Automatic Calling

Postamplification fluorescent melting curves were analyzed with the LC480 Gene Scanning software v1.2.9 (Roche Diagnostics Corporation). All curves were analyzed after normalization, temperature shifting, automated grouping, and the inspection of difference plots. Normalization was performed to remove any background fluorescence from the melting curve and the results were rescaled from 0 to 100% annealed. Temperature shifting was performed to align the fluorescence readings at 5% annealed (setting of automatic calling at 5). This level was chosen to correct for instrument and temperature variability across the melting block while maintaining differences in the melting profiles. The grouping software uses a curve shape-matching algorithm to identify wild type from mutant samples and cutoffs are based on variability from the wild-type curve. The wild-type and test samples were of the same preparation type. Grouping sensitivities of 0.20, 0.15, and 0.10 were compared to determine optimal mutation calling on the LightCycler 480 (see Results section). Higher sensitivity settings tolerate less variability in the melting curves for calling a positive result. As a cross reference, groupings were verified by inspection of the difference plots.

Direct Sequencing

Samples were prepared for direct sequencing using sequencing-specific primers spanning the scanning regions (Supplementary Table S2). Amplification with the sequencing primers was performed in a final reaction volume of 20 μl containing 1 × PCR buffer 3 (Idaho Technology), 10 ng DNA, 0.5 μM each of forward and reverse primers, 0.2 mM each of dNTP (Applied

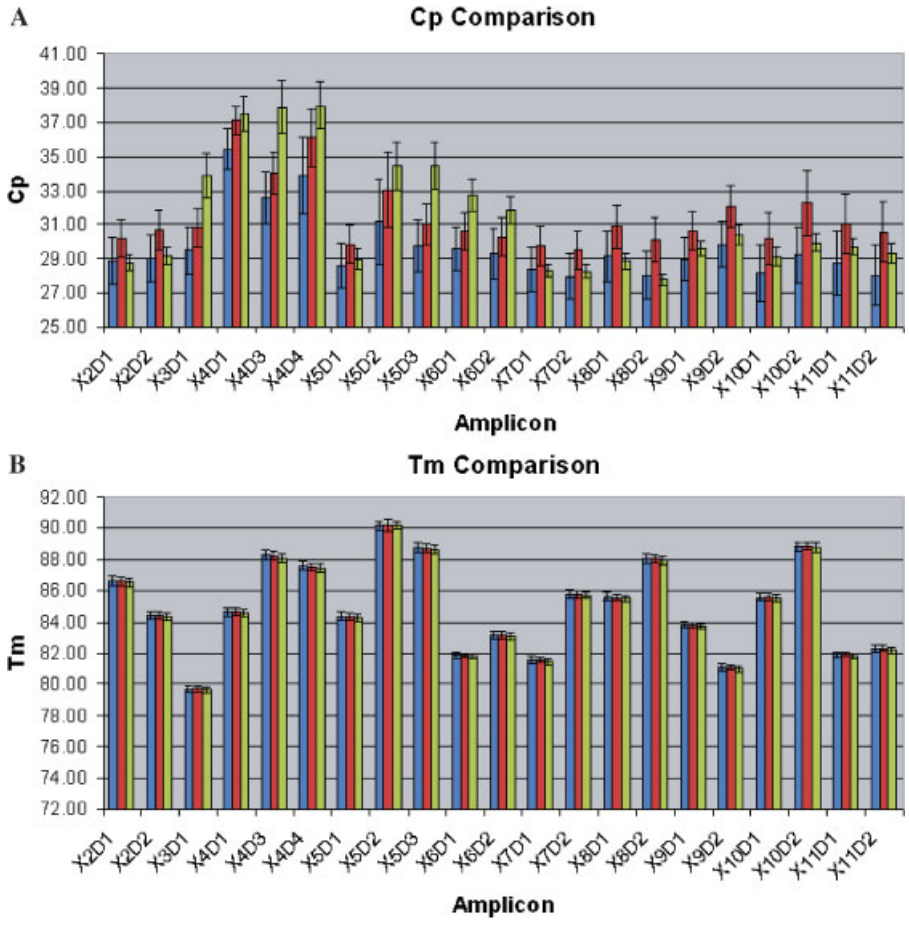

FIGURE 1. **Comparison of crossing points (Cps) and melting temperatures (Tms) across three different DNA preparation methods. DNA was extracted from FF and FFPE tissue on 14 samples and each scanning amplicon (21 total) was compared for variation in Cps (A) and Tms (B). A comparison was made between FF (blue bars), FFPE (red bars), and WGA DNA (green bars) from the FF tissue. The confidence intervals are shown for 2 standard deviations from the mean. Although amplicons between the methods can have significantly different Cps, there is no difference in the Tms.**

Biosystems, Foster City, CA), and 0.2 U Platinum Taq (Invitrogen, Carlsbad, CA). PCR was carried out in the LightCycler (Roche Diagnostics Corporation) using an initial denaturation step (95°C for 5 min) followed by 50 cycles of denaturation (94°C for 3 s), annealing (58°C for 6 s), and extension (72°C for 6 s). Samples were then diluted 1:5 with water and 1 µl was used for sequencing. Sequencing was performed by dideoxynucleotide chain termination on a 48-capillary ABI 3730 instrument (Applied Biosystems). Sequences were analyzed using Sequencher version 4.5 (Gene Codes, Ann Arbor, MI). Mutations detected were numbered based on the cDNA sequence for TP53 (NCBI RefSeq NM_000546.3) and numbered with reference to +1 as the A of the ATG translation start codon (www.hgvs.org/mutnomen).

RESULTS

Sensitivity and Specificity of Scanning From Different DNA Preparations

We used LC480 Gene Scanning software to automatically call TP53 mutation status from PCR amplicon fluorescent melting curves. Sensitivity and specificity of scanning was compared to direct sequencing at different "group sensitivity" thresholds set by the instrument software. The results from sequencing were blinded until analyses were complete. A set of 14 breast samples were completely sequenced and scanned for mutations in TP53 using DNA prepared from FF (WGA and non-WGA) and FFPE tissue. Table 1 shows optimal "group sensitivities" (bold) for scanning using different DNA preparations. There was 100% sensitivity and 99% specificity for calling mutations using non-WGA amplified DNA from fresh tissue (optimal grouping sensitivity 0.2). Although the specificity remained high for scanning WGA DNA from fresh tissue (95% specificity) and DNA from FFPE tissue (100% specificity), the sensitivity decreased to 86% for both these preparations (optimal grouping sensitivity 0.15).

The Effect of Cp on Melting Temperature (Tm)

Since amplicon sequence, length, and concentration can affect the melting temperature (Tm) of the PCR product and the ability to detect mutations, we analyzed the variation in Cp and Tm for each amplicon across the preparation methods using a common set of samples (Fig. 1). Although the calculated input for each sample was the same (10 ng DNA), we found that the different preparation methods resulted in significantly different amplicon Cps (Fig. 1A). Importantly, the differences in Cps between the methods did not result in a significant change in Tm (Fig. 1B). Finally, differences in Cps across the methods were compared with GC content (Supplementary Table S1) and, while some high GC amplicons associated with Cp differences in WGA samples, there was no consistent trend.

Mutation Detection by Scanning and Direct Sequencing

We used a set of 23 samples that had complete scanning (483 amplicons) and sequencing to establish an optimal "grouping sensitivity" for FF tissue DNA (Table 1). We then used this optimal cutoff to automatically call mutations in an additional 55 FF breast samples scanned for the entire TP53 coding region. Out of 55 samples and 1,155 amplicons scanned, there were 27 samples flagged for alterations. Direct sequencing of those

TABLE 2. TP53 Alterations Detected*

Sample	Amplicon	Exon	Codon	Mutation[a]	Protein	Domain	Activity[b]
UB37	X2D1	2	2	c.6G>A	p.(=)	Transactivation	Unknown
UB95	X4D1	4	36	c.108G>A	p.(=)	Transactivation	Normal
UB131	X4D1	4	41	c.121_124delGATG	p.Asp41IlefsX2	Transactivation	Unknown
UB116	X4D3, X4D4	4	102	c.304dupA	p.Thr102AsnfsX29	DNA binding	Unknown
PB126	X4D4	4	107	c.321delC	p.Tyr107X	DNA binding	Unknown
UB29	X5D2	5	141	c.422G>A	p.Cys141Tyr	DNA binding/S3	9.84
UB37	X5D2	5	165	c.493C>T	p.Gln165X	DNA binding/L2	0
SKBR3[c]	X5D3	5	175	c.524G>A	p.Arg175His	DNA binding/L2	12.41
PB297	X5D3	5	175	c.524G>A	p.Arg175His	DNA binding/L2	12.41
PB441	X6D2	6	206	c.618G>A	p.(=)	DNA binding/S6	Unknown
UB78[d]	X6D2	6	213	c.639A>G	p.(=)	DNA binding domain	Normal
UB78LN[d]	X6D2	6	213	c.639A>G	p.(=)	DNA binding domain	Normal
UB64	X6D2	6	213	c.639A>G	p.(=)	DNA binding domain	Normal
UB45	X6D2	6	213	c.639A>G	p.(=)	DNA binding domain	Normal
UB120[d]	X6D2	6	216	c.646G>A	p.Val216Met	DNA binding/S7	0.16
UB120LN[d]	X6D2	6	216	c.646G>A	p.Val216Met	DNA binding/S7	0.16
UB110	X6D2	6	220	c.659A>G	p.Tyr220Cys	DNA binding	1.21
PB205	X7D1	i6	Intronic	c.7–1G>A	p.?	Splice Acceptor Site	Unknown
PB376	X7D2	7	257	c.770T>A	p.Leu257Gln	DNA binding/S9	10.96
UB60	X8D1	8	261	c.783delT	p.Ser261ArgfsX115	DNA binding	Unknown
PB268	X8D1	8	270	c.810T>A	p.Phe270Leu	DNA binding/S10	8.14
PB268	X8D1	8	271	c.811delG	p.Glu271ArgfsX110	DNA binding/S10	Unknown
UB25	X8D1	8	273	c.818G>C	p.Arg273Pro	DNA binding	0.58
UB71	X8D1, X8D2	8	280	c.839G>A	p.Arg280Lys	DNA binding/H2	0.46
BT474[c]	X8D2	8	285	c.853G>A	p.Glu285Lys	DNA binding/H2	0.58
UB43	X8D2	8	290	c.869G>A	p.Arg290His	DNA binding	67.3
UB95	X9D2	i9	Intronic	c.9+13T>C	p.(=)	Intronic	Unknown
PB419	X10D1	10	333	c.998_999delGT	p.Arg333ArgfsX3	Oligomerization	Unknown
UB43	X10D1	10	337	c.1010G>T	p.Arg337Leu	Oligomerization	10.45
UB118	X10D1	10	342	c.1024C>T	p.Agr342X	Oligomerization	0
PB138	X10D1	10	342	c.1024C>T	p.Agr342X	Oligomerization	0
UB44	X10D2	i10	Intronic	c.10+30A>T	p.(=)	Intronic	Unknown

*RefSeq NM.000546.3.
[a]Number based on cDNA sequence, +1 as A of ATG start codon.
[b]Based on percent functional activity from in-vitro assays [Kato et al., 2003].
[c]Cell lines with known alterations.
[d]Matched primary and lymph node (LN) samples.

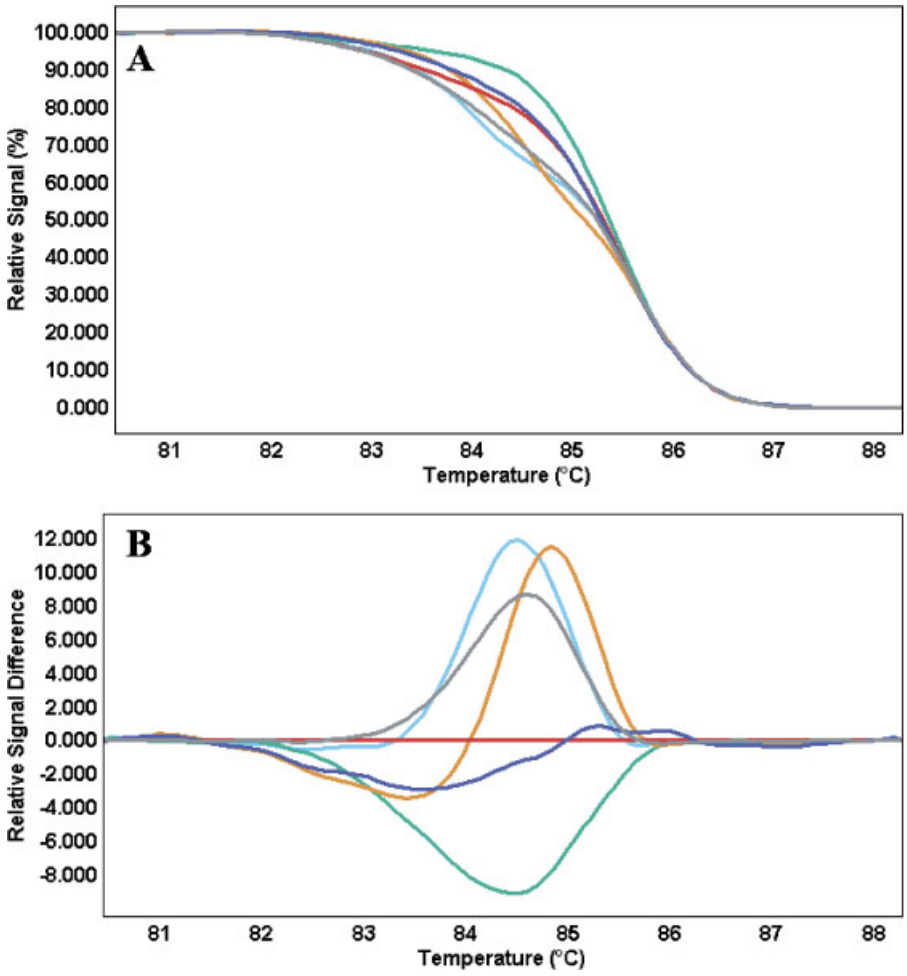

FIGURE 2. **Distinguishing multiple types of mutations within an amplicon. Fluorescence-normalized and temperature-corrected melting curves (A) and difference plots (B) are shown for five samples (UB60-green, PB268-gray, UB25-turquoise, UB71-orange, and BT474-blue) and a wild-type control (red). Scanning is able to resolve a spectrum of different mutations, including three point mutations in different codons (UB25, UB71, and BT474), a single base pair deletion (UB60), and a complex mutation (PB268).**

amplicons confirmed mutations/polymorphisms in 23 samples (85% accuracy).

Table 2 presents all the variants (polymorphisms and mutations) found by scanning and confirmed by sequencing. There were two patients with mutations detected in matched primary tumor and lymph node samples (UB78/UB78LN and UB120/UB120LN). Two samples had mutations detected by overlapping amplicons (UB116 detected by X4D3 and X4D4; UB71 detected by X8D1 and X8D2). A total of three samples had two variants detected by different scanning amplicons (UB37, UB43, and UB95). Sample PB268 had a complex mutation comprised of both a single-base change and a base deletion in adjacent codons. A total of six of the variants detected represent known polymorphisms with five occurring at codon 213. In addition to the polymorphisms, we detected 13 missense mutations, six frameshift mutations, three nonsense mutations, two silent mutations, and three intronic variations. Figure 2 shows high-resolution fluorescent melting curve profiles for five different mutations within exon 8 of TP53.

Limits of Detection

Since tissue heterogeneity and sampling error are potential sources of false negatives in tumors, we assessed the ability to detect DNA mutations in a background of wild type. Figure 3 shows mutant TP53 DNA from the BT474 cell line, carrying the E285K (853G>A) homozygous mutation, serially diluted into a background of wild-type TP53 DNA from the MCF7 cell line. Dilutions from 1:1 to 1:200 were assayed in triplicate. Manual inspection of the absolute Tm and the shape of the melting curves in Figure 3A and B show that the largest difference in the plots are between the very low and very high dilutions. This is clearly seen in the difference plot (Fig. 3C) that shows the 1:5, 1:10, and 1:20 dilutions approaching the wild-type curve and then the higher dilutions becoming more aberrant again. The mutant cell line alone (BT474) shows only a small deviation from the wild-type alone curve because both are forming homoduplexes. Since each alteration may have a different limit of detection and dilution profile, we also performed dilutions with the cell line SKBR3 (loss of heterozygosity at exon 4, R175H) and found similar results (data not shown).

DISCUSSION

Comprehensive resequencing efforts are identifying many potential cancer genes that will need to be further examined to determine their frequency and distribution across histological types [Sjoblom et al., 2006]. High-throughput scanning assays that can

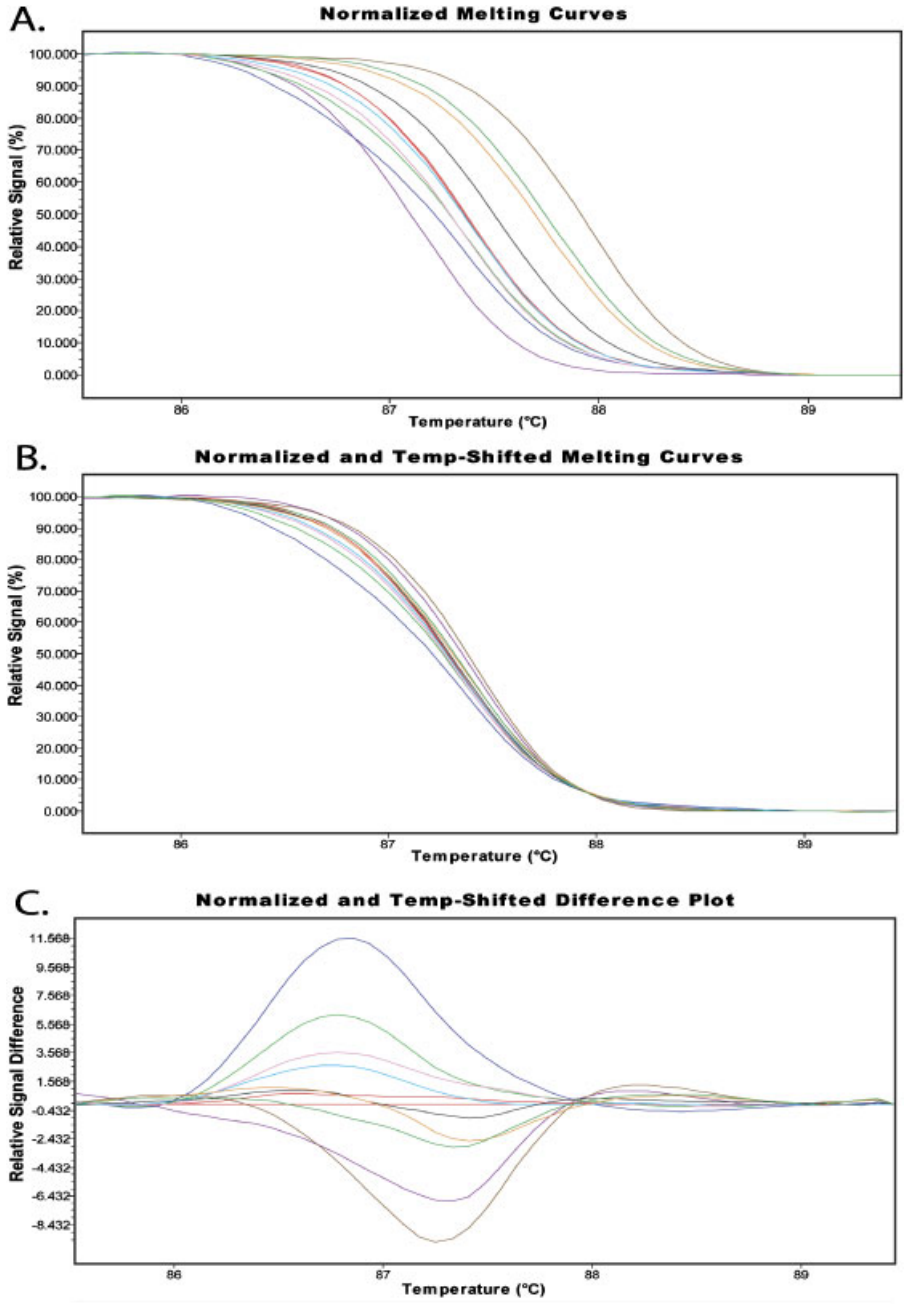

FIGURE 3. **Limits of detection for scanning. Fluorescent melting curves without temperature correction (A) and with temperature correction (B) allow for interpretation of the melting temperature and shape of the curves. Wild-type DNA from the cell line MCF7 (red in duplicate) is compared to mutated DNA from the cell line BT474 alone (purple) and at serial dilutions (1:1-blue, 1:2-light green, 1:5-pink, 1:10-turquoise, 1:20-black, 1:50-orange, 1:100-dark green, and 1:200-brown). There is little difference in the shape of the melting curves for the wild-type DNA (MCF7) and homozygous mutated DNA (BT474) since both form homoduplexes. The mutations become more apparent on the difference plot (C). In order to show the "normal" variation in the fluorescent melting curves, we selected one of the normal duplicates to serve as a reference in the difference plot and included the other as a test sample.**

be automated are invaluable to this research. In addition, assays that can be performed from archived tissue (i.e., FFPE) and/or limited sample are particularly appealing since they can be used in both retrospective studies and within the current framework of specimen processing in clinical pathology.

Previous work has shown that large regions of fresh tissue DNA can be scanned by high-resolution fluorescent melting curve analyses using the dsDNA dyes LC Green or SYTO9 (Invitrogen) [Herrmann et al., 2006; Krypuy et al., 2007; Wittwer et al., 2003]. This technology has also been used to detect sporadic mutations in "hotspots" for several different cancer genes using DNA from FFPE tissues [Willmore-Payne et al., 2006a, 2006b].

Our work shows automation of high-resolution fluorescent melting curve analyses done in a 384-well format with automatic mutation calling. The assay had high sensitivity/specificity for scanning the TP53 gene from several different DNA preparation types (FF, WGA, and FFPE). We saw the highest sensitivity using FF DNA, although this was based on agreement to direct

sequencing performed on the same specimen type. Thus, sampling differences could account for some discordance between sequencing results from FF tissue and scanning results from FFPE tissue.

Regions of the genome that are not well represented, due to biases in whole genome amplification or susceptibility to fragmentation by formalin fixation, will have later Cps. We have shown that variability in Cp does not significantly change Tm, however very late Cps (i.e., >40) that are a result of limited starting copy number could potentially be a source of discordance if only the wild-type copy is amplified.

Because tumor samples are heterogenous and may contain varying amounts of normal cells and even different populations of malignant cells, it is important clinically to determine the limits of detection for a scanning assay. We found by mixing experiments that we could detect mutant TP53 DNA present as low as 0.5% in a background of wild-type DNA. This may explain the apparent overcalling of mutations by scanning since standard dideoxynucleotide chain termination (i.e., Sanger) sequencing only detects down to about 1:10. For comparison, custom microarray chips designed to determine alterations at each base of TP53 have shown high sensitivity but low specificity and limits of detection as low as 1% [Wikman et al., 2000]. Another technology that could nicely complement scanning by high resolution fluorescent melting curves is emulsion pyrosequencing, which has been reported to detect variants in proportions as low as 0.2% [Thomas et al., 2006].

There is convincing evidence from breast cancer studies that a sequence confirmed mutation in the TP53 gene indicates a poor prognosis independent of standard clinical parameters (tumor size, node status, and estrogen receptor [ER]-status) [Olivier et al., 2006]. Furthermore, TP53 mutations affecting the loop domains L2 and L3 have been associated with lack of response to standard chemotherapies in breast cancer [Geisler et al., 2001, 2003]. Interestingly, certain subtypes of breast cancer with a confirmed TP53 mutation may have an exceptionally good response to particular chemotherapy regimens. For example, patients with the Basal-like subtype of breast cancer harboring a TP53 mutation have shown to respond to a dose-dense epirubicin-cyclophosphamide drug regimen [Bertheau et al., 2007]. Perhaps the greatest promise for treating patients with p53 mutations will be in restoring wild-type p53 activity by adenovirus therapy or other targeted therapies [Bykov et al., 2002; Roth, 2006]. To date, trials conducted with p53 adenovirus therapy have shown to be safe and effective [Senzer et al., 2007], but larger prospective studies are needed.

Most reports of TP53 mutations focus only on the DNA binding domain (exons 5–8) because initial studies showed that most alterations occur in that region [Ory et al., 1994; Pavletich et al., 1993]. Unfortunately, this can lead to an overestimation of mutation frequency in exons 5–8 and lack of appreciation for the clinical significance of mutations occurring in exons 2–4 and 9–11. In this study, we were able to scan the entire coding region of TP53 with the exception of a 53-bp region in exon 4 that gave inconsistent PCR amplification. A total of 11 out of 27 (41%) alterations, not including polymorphisms, were found outside of exons 5–8. The function and activity of most of those mutations are unknown.

Functional assays combined with scanning and sequencing efforts are providing a better understanding of the biological relevance of different TP53 mutations [Kato et al., 2003]. Our TP53 scanning assay, together with databases that provide information on clinical and biological significance [Petitjean et al., 2007a, 2007b], should allow for accurate clinical interpretation to help guide therapeutic decision making for breast cancer and other cancers.

ACKNOWLEDGMENTS

This work was supported by the ARUP Institute for Clinical and Experimental Pathology, the Huntsman Cancer Institute/Foundation, and NCI grants R33-CA97769-01 (P.S.B.) and P50-CA58223-09A1 (C.M.P.). We thank Drs. Carl Wittwer and David Eyre for help with software support. We appreciate the support of the core facilities for tissue procurement at the participating institutions.

REFERENCES

Aas T, Borresen AL, Geisler S, Smith-Sorensen B, Johnsen H, Varhaug JE, Akslen LA, Lonning PE. 1996. Specific P53 mutations are associated with de novo resistance to doxorubicin in breast cancer patients. Nat Med 2:811–814.

Ahrendt SA, Halachmi S, Chow JT, Wu L, Halachmi N, Yang SC, Wehage S, Jen J, Sidransky D. 1999. Rapid p53 sequence analysis in primary lung cancer using an oligonucleotide probe array. Proc Natl Acad Sci USA 96:7382–7387.

Allred DC, Clark GM, Elledge R, Fuqua SA, Brown RW, Chamness GC, Osborne CK, McGuire WL. 1993. Association of p53 protein expression with tumor cell proliferation rate and clinical outcome in node-negative breast cancer. J Natl Cancer Inst 85:200–206.

Bergh J, Norberg T, Sjogren S, Lindgren A, Holmberg L. 1995. Complete sequencing of the p53 gene provides prognostic information in breast cancer patients, particularly in relation to adjuvant systemic therapy and radiotherapy. Nat Med 1:1029–1034.

Berns EM, Foekens JA, Vossen R, Look MP, Devilee P, Henzen-Logmans SC, van Staveren IL, van Putten WL, Inganas M, Meijer-van Gelder ME, Cornelisse C, Claassen CJ, Portengen H, Bakker B, Klijn JG. 2000. Complete sequencing of TP53 predicts poor response to systemic therapy of advanced breast cancer. Cancer Res 60:2155–2162.

Bertheau P, Turpin E, Rickman DS, Espie M, de Reynies A, Feugeas JP, Plassa LF, Soliman H, Varna M, de Roquancourt A, Lehmann-Che J, Beuzard Y, Marty M, Misset JL, Janin A, de The H. 2007. Exquisite sensitivity of TP53 mutant and basal breast cancers to a dose-dense epirubicin-cyclophosphamide regimen. PLoS Med 4:e90.

Borresen AL, Hovig E, Smith-Sorensen B, Malkin D, Lystad S, Andersen TI, Nesland JM, Isselbacher KJ, Friend SH. 1991. Constant denaturant gel electrophoresis as a rapid screening technique for p53 mutations. Proc Natl Acad Sci USA 88:8405–8409.

Borresen-Dale AL. 2003. TP53 and breast cancer. Hum Mutat 21: 292–300.

Bykov VJ, Issaeva N, Shilov A, Hultcrantz M, Pugacheva E, Chumakov P, Bergman J, Wiman KG, Selivanova G. 2002. Restoration of the tumor suppressor function to mutant p53 by a low-molecular-weight compound. Nat Med 8:282–288.

Elledge RM, Gray R, Mansour E, Yu Y, Clark GM, Ravdin P, Osborne CK, Gilchrist K, Davidson NE, Robert N, Tormey DC, Allred DC. 1995. Accumulation of p53 protein as a possible predictor of response to adjuvant combination chemotherapy with cyclophosphamide, methotrexate, fluorouracil, and prednisone for breast cancer. J Natl Cancer Inst 87:1254–1256.

Geisler S, Lonning PE, Aas T, Johnsen H, Fluge O, Haugen DF, Lillehaug JR, Akslen LA, Borresen-Dale AL. 2001. Influence of TP53 gene alterations and c-erbB-2 expression on the response to treatment with doxorubicin in locally advanced breast cancer. Cancer Res 61:2505–2512.

Geisler S, Borresen-Dale AL, Johnsen H, Aas T, Geisler J, Akslen LA, Anker G, Lonning PE. 2003. TP53 gene mutations predict the response to neoadjuvant treatment with 5-fluorouracil and mitomycin in locally advanced breast cancer. Clin Cancer Res 9:5582–5588.

Hainaut P, Hollstein M. 2000. p53 and human cancer: the first ten thousand mutations. Adv Cancer Res 77:81–137.

Herrmann MG, Durtschi JD, Bromley LK, Wittwer CT, Voelkerding KV. 2006. Amplicon DNA melting analysis for mutation scanning and genotyping: cross-platform comparison of instruments and dyes. Clin Chem 52:494–503.

Hollstein M, Sidransky D, Vogelstein B, Harris CC. 1991. p53 mutations in human cancers. Science 253:49–53.

Kato S, Han SY, Liu W, Otsuka K, Shibata H, Kanamaru R, Ishioka C. 2003. Understanding the function-structure and function-mutation relationships of p53 tumor suppressor protein by high-resolution missense mutation analysis. Proc Natl Acad Sci USA 100:8424–8429.

Krypuy M, Ahmed AA, Etemadmoghadam D, Hyland SJ, Group AO, Brenton JD, Fox SB, Defazio A, Bowtell DD, Dobrovic A. 2007. High resolution melting for mutation scanning of TP53 exons 5–8. BMC Cancer 7:168.

Le Calvez F, Ahman A, Tonisson N, Lambert J, Temam S, Brennan P, Zaridze DG, Metspalu A, Hainaut P. 2005. Arrayed primer extension resequencing of mutations in the TP53 tumor suppressor gene: comparison with denaturing HPLC and direct sequencing. Clin Chem 51:1284–1287.

Legros Y, Meyer A, Ory K, Soussi T. 1994. Mutations in p53 produce a common conformational effect that can be detected with a panel of monoclonal antibodies directed toward the central part of the p53 protein. Oncogene 9:3689–3694.

Levine AJ, Momand J, Finlay CA. 1991. The p53 tumour suppressor gene. Nature 351:453–456.

Levine AJ. 1997. p53, the cellular gatekeeper for growth and division. Cell 88:323–331.

MacGrogan G, Mauriac L, Durand M, Bonichon F, Trojani M, de Mascarel I, Coindre JM. 1996. Primary chemotherapy in breast invasive carcinoma: predictive value of the immunohistochemical detection of hormonal receptors, p53, c-erbB-2, MiB1, pS2 and GST pi. Br J Cancer 74:1458–1465.

Malkin D, Li FP, Strong LC, Fraumeni JF, Jr, Nelson CE, Kim DH, Kassel J, Gryka MA, Bischoff FZ, Tainsky MA, Friend S. 1990. Germ line p53 mutations in a familial syndrome of breast cancer, sarcomas, and other neoplasms. Science 250:1233–1238.

Miller LD, Smeds J, George J, Vega VB, Vergara L, Ploner A, Pawitan Y, Hall P, Klaar S, Liu ET, Bergh J. 2005. An expression signature for p53 status in human breast cancer predicts mutation status, transcriptional effects, and patient survival. Proc Natl Acad Sci USA 102:13550–13555.

Millward H, Samowitz W, Wittwer CT, Bernard PS. 2002. Homogeneous amplification and mutation scanning of the p53 gene using fluorescent melting curves. Clin Chem 48:1321–1328.

Moore L, Godfrey T, Eng C, Smith A, Ho R, Waldman FM. 2000. Validation of fluorescent SSCP analysis for sensitive detection of p53 mutations. Biotechniques 28:986–992.

Olivier M, Eeles R, Hollstein M, Khan MA, Harris CC, Hainaut P. 2002. The IARC TP53 database: new online mutation analysis and recommendations to users. Hum Mutat 19:607–614.

Olivier M, Langerod A, Carrieri P, Bergh J, Klaar S, Eyfjord J, Theillet C, Rodriguez C, Lidereau R, Bieche I, Varley J, Bignon Y, Uhrhammer N, Winqvist R, Jukkola-Vuorinen A, Niederacher D, Kato S, Ishioka C, Hainaut P, Borresen-Dale AL. 2006. The clinical value of somatic TP53 gene mutations in 1,794 patients with breast cancer. Clin Cancer Res 12:1157–1167.

Ory K, Legros Y, Auguin C, Soussi T. 1994. Analysis of the most representative tumour-derived p53 mutants reveals that changes in protein conformation are not correlated with loss of transactivation or inhibition of cell proliferation. EMBO J 13:3496–3504.

Pavletich NP, Chambers KA, Pabo CO. 1993. The DNA-binding domain of p53 contains the four conserved regions and the major mutation hot spots. Genes Dev 7:2556–2564.

Petitjean A, Achatz MI, Borresen-Dale AL, Hainaut P, Olivier M. 2007a. TP53 mutations in human cancers: functional selection and impact on cancer prognosis and outcomes. Oncogene 26:2157–2165.

Petitjean A, Mathe E, Kato S, Ishioka C, Tavtigian SV, Hainaut P, Olivier M. 2007b. Impact of mutant p53 functional properties on TP53 mutation patterns and tumor phenotype: lessons from recent developments in the IARC TP53 database. Hum Mutat 28:622–629.

Roth JA. 2006. Adenovirus p53 gene therapy. Expert Opin Biol Ther 6:55–61.

Rozan S, Vincent-Salomon A, Zafrani B, Validire P, De Cremoux P, Bernoux A, Nieruchalski M, Fourquet A, Clough K, Dieras V, Pouillart P, Sastre-Garau X. 1998. No significant predictive value of c-erbB-2 or p53 expression regarding sensitivity to primary chemotherapy or radiotherapy in breast cancer. Int J Cancer 79:27–33.

Santibanez-Koref MF, Birch JM, Hartley AL, Jones PH, Craft AW, Eden T, Crowther D, Kelsey AM, Harris M. 1991. p53 germline mutations in Li-Fraumeni syndrome. Lancet 338:1490–1491.

Senzer N, Nemunaitis J, Nemunaitis M, Lamont J, Gore M, Gabra H, Eeles R, Sodha N, Lynch FJ, Zumstein LA, Menander KB, Sobol RE, Chada S. 2007. p53 therapy in a patient with Li-Fraumeni syndrome. Mol Cancer Ther 6:1478–1482.

Sjoblom T, Jones S, Wood LD, Parsons DW, Lin J, Barber TD, Mandelker D, Leary RJ, Ptak J, Silliman N, Szabo S, Buckhaults P, Farrell C, Meeh P, Markowitz SD, Willis J, Dawson D, Willson JK, Gazdar AF, Hartigan J, Wu L, Liu C, Parmigiani G, Park BH, Bachman KE, Papadopoulos N, Vogelstein B, Kinzler KW, Velculescu VE. 2006. The consensus coding sequences of human breast and colorectal cancers. Science 314:268–274.

Soong R, Iacopetta BJ, Harvey JM, Sterrett GF, Dawkins HJ, Hahnel R, Robbins PD. 1997. Detection of p53 gene mutation by rapid PCR-SSCP and its association with poor survival in breast cancer. Int J Cancer 74:642–647.

Sorlie T, Perou CM, Tibshirani R, Aas T, Geisler S, Johnsen H, Hastie T, Eisen MB, van de Rijn M, Jeffrey SS, Thorsen T, Quist H, Matese JC, Brown PO, Botstein D, Lonning PE, Borresen-Dale AL. 2001. Gene expression patterns of breast carcinomas distinguish tumor subclasses with clinical implications. Proc Natl Acad Sci USA 98:10869–10874.

Sorlie T, Johnsen H, Vu P, Lind GE, Lothe R, Borresen-Dale AL. 2005. Mutation screening of the TP53 gene by temporal temperature gradient gel electrophoresis. Methods Mol Biol 291:207–216.

Soussi T, Beroud C. 2001. Assessing TP53 status in human tumours to evaluate clinical outcome. Nat Rev Cancer 1:233–240.

Thomas RK, Nickerson E, Simons JF, Janne PA, Tengs T, Yuza Y, Garraway LA, LaFramboise T, Lee JC, Shah K, O'neill K, Sasaki H, Lindeman N, Wong KK, Borras AM, Gutmann EJ, Dragnev KH, DeBaisi R, Chen TH, Glatt KA, Greulich H, Desany B, Lubeski CK, Brockman W, Alvarez P, Hutchison SK, Leamon JH, Ronan MT, Turenchalk GS, Egholm M, Sellers WR, Rothberg JM, Meyerson M. 2006. Sensitive mutation detection in heterogeneous cancer specimens by massively parallel picoliter reactor sequencing. Nat Med 12:852–855.

Tonisson N, Zernant J, Kurg A, Pavel H, Slavin G, Roomere H, Meiel A, Hainaut P, Metspalu A. 2002. Evaluating the arrayed primer extension resequencing assay of TP53 tumor suppressor gene. Proc Natl Acad Sci USA 99:5503–5508.

Wikman FP, Lu ML, Thykjaer T, Olesen SH, Andersen LD, Cordon-Cardo C, Orntoft TF. 2000. Evaluation of the performance of a p53 sequencing microarray chip using 140 previously sequenced bladder tumor samples. Clin Chem 46:1555–1561.

Willmore-Payne C, Holden JA, Chadwick BE, Layfield LJ. 2006a. Detection of c-kit exons 11- and 17-activating mutations in testicular seminomas by high-resolution melting amplicon analysis. Mod Pathol 19:1164–1169.

Willmore-Payne C, Holden JA, Layfield LJ. 2006b. Detection of epidermal growth factor receptor and human epidermal growth factor receptor 2 activating mutations in lung adenocarcinoma by high-resolution melting amplicon analysis: correlation with gene copy number, protein expression, and hormone receptor expression. Hum Pathol 37:755–763.

Wittwer CT, Reed GH, Gundry CN, Vandersteen JG, Pryor RJ. 2003. High-resolution genotyping by amplicon melting analysis using LCGreen. Clin Chem 49:853–860.